


Proceedings Article

An effective reconstruction method for magnetic particle imaging based on deep neural networks constrained by a physical model

Pengfei Huang ^{a,b} · Shenghan Ren^{a,b} · Yu Meng^{a,b} · Zhonghao Zhang^{a,b} · Duofang Chen^{a,b} · Shouping Zhu ^b · Xueli Chen^{a,b*}

^aBiomedical-photonics and Molecular Imaging Laboratory, School of Life Science and Technology, Xidian University & Engineering Research Center of Molecular and Neuro Imaging, Ministry of Education, Xi'an, Shaanxi 710126, China.

^bXi'an Key Laboratory of Intelligent Sensing and Regulation of trans-Scale Life Information & International Joint Research Center for Advanced Medical Imaging and Intelligent Diagnosis and Treatment, School of Life Science and Technology, Xidian University, Xi'an, Shaanxi 710126, China.

*Corresponding author, email: xlchen@xidian.edu.cn

© 2023 Huang *et al.*; licensee Infinite Science Publishing GmbH

This is an Open Access article distributed under the terms of the Creative Commons Attribution License (<http://creativecommons.org/licenses/by/4.0>), which permits unrestricted use, distribution, and reproduction in any medium, provided the original work is properly cited.

Abstract

Magnetic particle imaging (MPI) visualizes the spatial distribution of magnetic particles based on their nonlinear response signals. Such a process can be implemented by image reconstruction. In recent years, deep learning techniques supported by large amounts of training data have been widely used in various medical image reconstructions. However, the acquisition of MPI data requires a long time of obtaining and preprocessing. This makes it impractical to obtain a sufficient amount of data for training. In this work, we propose an MPI image reconstruction framework that incorporates physical model constraints into deep learning networks to overcome the limitation of dependence on training data. This framework optimizes the network parameters through constraints of the physical model rather than training with paired data. Simulation results show that this is an effective reconstruction strategy and has good reconstruction robustness.

1. Introduction

Similar to molecular imaging techniques such as positron emission tomography, emerging magnetic particle imaging (MPI) is a technique for quantitative visualization of magnetic nanoparticles (MNPs) distribution *in vivo*, and thus can respond to living biological processes at the cellular or molecular level. In MPI, the spatial distribution and concentration of MNPs are obtained by a reconstruction based on the measured volt-

age signal. System-matrix-based reconstruction[1] and x-space reconstruction[2] are two primarily used reconstruction algorithms for MPI. In recent years, deep learning (DL) techniques have been used for MPI reconstruction. The vast majority of the DL-enabled MPI reconstruction methods use supervised training strategies [3, 4] and thus require a large amount of training data to optimize the network parameters. It is difficult for MPI to collect a large amount of measurement data and the corresponding ground truth used for reconstruction. Deep

image prior (DIP) has been used to solve this problem in MPI[5]. However, DIP requires proper architecture and stopping criterion to obtain high-quality reconstruction results[6].

In this paper, we propose an MPI image reconstruction framework that incorporates physical model constraints into DL networks, allowing reconstruction to proceed without any training data. Different from the conventional DL networks, the proposed framework integrates a physical model for generating voltage signals from the spatial distribution of MNPs. This physical model is based on the MPI system function to calculate the voltage from the reconstruction results of DL networks. The errors between the results calculated by the physical model and the measured voltage are used to optimize the weights and biases via gradient descent. This will drive the constraint reconstruction results of the network towards the real spatial distribution of MNPs as the iterative process proceeds. We add regularization terms to the network loss function compared with DIP. This makes the proposed method not require a complex network structure and a proper number of iterations.

II. Theory

II.I. Neural Network

In the proposed framework, the first step is to generate the concentration distribution of MNPs using a fully connected network:

$$\hat{\mathbf{c}} = \varphi_{\theta}(\mathbf{z}). \quad (1)$$

Where φ_{θ} represents the neural network to reconstruct the MNPs distribution from the input $\mathbb{R}^z \rightarrow \mathbb{R}^N$, θ represents the network parameters, \mathbf{z} represents the input of the network, and $\hat{\mathbf{c}}$ representing the reconstructed MNPs distribution is the output of the network. Here, the network input uses a constant vector, and the network outputs the MNPs distribution using multiple fully connected layers.

II.II. Physical Model

The physical model is used to calculate the voltage signal from the MNPs concentration generated by the model(1). In this work, we selected the system matrix as the physical model:

$$\mathbf{u} = \mathbf{S}\mathbf{c}, \quad (2)$$

where $\mathbf{c} \in \mathbb{R}^N$ denotes the frequency spectrum of the voltage, $\mathbf{S} \in \mathbb{R}^{M \times N}$ is system matrix.

II.III. Loss Function

The loss function we use consists of two parts. The first part is the mean absolute error (MAE) between the mea-

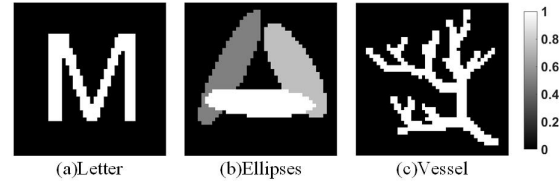


Figure 1: Phantoms used for the simulation.

sured voltage and the voltage calculated by the physical model:

$$L_u = \|\mathbf{P}(\varphi_{\theta}(\mathbf{z})) - \mathbf{u}_{meas}\|_1. \quad (3)$$

Where $\mathbf{P}(\cdot)$ represents the physical model, \mathbf{u}_{meas} is the measured voltage. In the second part, l_1 and total variation (TV) regularization terms are used to constrain the distribution of MNPs and improve the reconstruction quality. Therefore, the overall loss function can be expressed:

$$L = L_u + \alpha \|\hat{\mathbf{c}}\|_1 + \beta V(\hat{\mathbf{c}}). \quad (4)$$

Where $V(\cdot)$ represents the TV, α and β are hyperparameters to adjust the ratio between different parts of the loss.

III. Materials and Methods

III.I. Simulation Data

We investigated the reconstruction quality of the proposed framework by two-dimensional simulation data. The reconstruction result is compared to Tikhonov regularized Kaczmarz reconstruction method[7]. We set the number of iterations to 300 and adjust the regularization parameter as the value when the peak signal-to-noise ratio (PSNR) is the maximum.

Three different phantoms were designed to evaluate the reconstruction quality on different kinds of image structures (Fig. 1). We generated simulation data according to $\mathbf{u} = \mathbf{S}\mathbf{c} + \sigma$ [8], where \mathbf{c} denotes the ground truth and σ is a vector that adds white Gaussian noise to the voltage. The system matrix used in this study was taken from data provided by T. Knopp *et al.*[9]. Here, $N = 1936$ is the size of the ground truth. The sample positions have a distance of 1 mm. $M = 1372$ is the size of the selected frequency domain signal.

III.II. Network Training

The fully connected network was implemented on Python 3.8.0 platform using Pytorch version 1.11.0. We used the Adam optimizer to optimize the network parameters with a learning rate of 10^{-4} . 10000 epochs were used for each data to ensure a good reconstructed image.

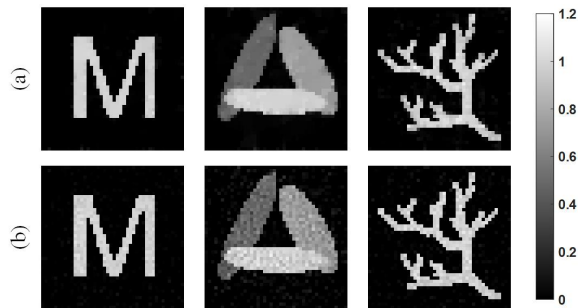


Figure 2: Comparisons between the proposed framework (a) and Kaczmarz reconstruction (b) for data added with 1% Gaussian noise.

Network training is performed on an NVIDIA TITAN GTX GPU.

IV. Results and Discussions

We first compared the reconstruction results of the three phantoms for the proposed framework and the Kaczmarz method (Fig. 2). 1% Gaussian white noise was added to the data. The results of the Kaczmarz method contain more noise, especially in the reconstruction of the elliptical phantom. Quantitatively comparing the reconstruction results of the two methods, we found that the Kaczmarz method overestimated the concentration of MNPs. In contrast, the reconstruction results of the proposed framework are less noisy and closer to the real MNPs concentration.

Next, we evaluated the robustness of the two methods regarding higher levels of noise. To do this, we added 3%, 5%, and 10% white Gaussian noise to the data, respectively. The reconstruction results are shown in Fig. 3. As the noise level increases, more noise is generated at the edges of the results produced by Kaczmarz. The proposed framework has higher noise immunity at 3% and 5% noise. However, when the noise level reaches 10%, it will cause the image edges to be too smooth.

Finally, we calculate the PSNR and structural similarity (SSIM) of the three phantoms at different noise levels (Table 1). For the reconstruction of the letter and the ellipses, the proposed framework provides better results, especially in the case of high levels of Gaussian noise. For the reconstruction of the vessel, Kaczmarz achieved a better reconstruction. This is probably due to the fact that the vessel has long image edges, while TV regularization is not good at dealing with these edges.

V. Conclusions

We propose an effective reconstruction method for magnetic particle imaging based on the integration of

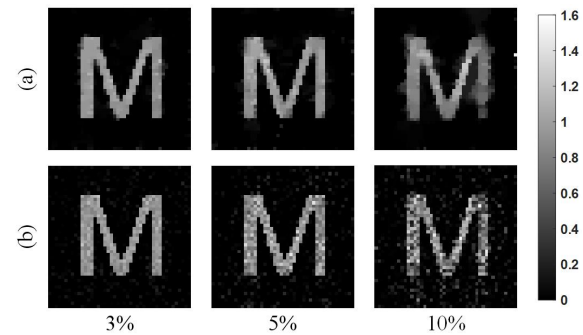


Figure 3: Comparison between the proposed framework (a) and Kaczmarz reconstruction (b) for data added with different levels of Gaussian noise.

Table 1: PSNR and SSIM of the reconstruction results

noise level			Letter	Ellipses	Vessel
1%	PSNR	KA	32.458	25.058	30.143
		Ours	35.013	28.878	27.387
	SSIM	KA	0.920	0.786	0.919
		Ours	0.990	0.905	0.939
3%	PSNR	KA	23.911	16.533	21.101
		Ours	24.900	22.026	18.898
	SSIM	KA	0.822	0.554	0.847
		Ours	0.927	0.800	0.830
5%	PSNR	KA	20.484	13.561	17.348
		Ours	22.742	18.351	16.241
	SSIM	KA	0.779	0.422	0.785
		Ours	0.888	0.676	0.810
10%	PSNR	KA	14.788	10.755	12.914
		Ours	16.373	15.710	12.625
	SSIM	KA	0.588	0.285	0.611
		Ours	0.728	0.548	0.623

deep neural networks with the physical model. The method optimizes network parameters through constraints based on physical models instead of training with a large amount of data. Simulation results showed excellent reconstruction results and noise immunity.

Acknowledgments

This work was supported in part by the National Key R&D Program of China (2022YFB3203800), the National Natural Science Foundation of China (61901338), the National Young Talent Program, the Shaanxi Science Fund for Distinguished Young Scholars (2020JC-27), the Shaanxi Young Top-notch Talent Program.

Author's statement

Conflict of interest: Authors state no conflict of interest.

References

- [1] T. Knopp, S. Biederer, T. F. Sattel, J. Rahmer, J. Weizenecker, B. Gleich, J. Borgert, and T. M. Buzug. 2d model-based reconstruction for magnetic particle imaging. *Medical Physics*, 37(2):485–491, 2010.
- [2] P. W. Goodwill and S. M. Conolly. The x-space formulation of the magnetic particle imaging process: 1-d signal, resolution, bandwidth, snr, sar, and magnetostimulation. *IEEE Transactions on Medical Imaging*, 29(11):1851, 2010.
- [3] B. G. Chae. Neural network image reconstruction for magnetic particle imaging. *ETRI Journal*, 39(6):841–850, 2017, doi:<https://doi.org/10.4218/etrij.2017-0094>.
- [4] B. Askin, A. Güngör, D. Alptekin Soydan, E. U. Saritas, C. B. Top, and T. Cukur. Pp-mpi: A deep plug-and-play prior for magnetic particle imaging reconstruction, in *Machine Learning for Medical Image Reconstruction*, N. Haq, P. Johnson, A. Maier, C. Qin, T. Würfl, and J. Yoo, Eds., 105–114, Cham: Springer International Publishing, 2022.
- [5] S. Dittmer, T. Kluth, M. Henriksen, and P. Maass. Deep image prior for 3d magnetic particle imaging: A quantitative comparison of regularization techniques on open mpi dataset, 2020. eprint: [arXiv:2007.01593](https://arxiv.org/abs/2007.01593).
- [6] T. Knopp and M. Grosser. Warmstart approach for accelerating deep image prior reconstruction in dynamic tomography, in *Proceedings of The 5th International Conference on Medical Imaging with Deep Learning*, E. Konukoglu, B. Menze, A. Venkataraman, C. Baumgartner, Q. Dou, and S. Albarqouni, Eds., ser. Proceedings of Machine Learning Research, 172, 713–725, PMLR, 2022.
- [7] T. Knopp, J. Rahmer, T. F. Sattel, S. Biederer, J. Weizenecker, B. Gleich, J. Borgert, and T. M. Buzug. Weighted iterative reconstruction for magnetic particle imaging. *Physics in Medicine & Biology*, 55(6):1577, 2010, doi:[10.1088/0031-9155/55/6/003](https://doi.org/10.1088/0031-9155/55/6/003).
- [8] M. Storath, C. Brandt, M. Hofmann, T. Knopp, J. Salamon, A. Weber, and A. Weinmann. Edge preserving and noise reducing reconstruction for magnetic particle imaging. *IEEE Transactions on Medical Imaging*, 36(1):74–85, 2017, doi:[10.1109/TMI.2016.2593954](https://doi.org/10.1109/TMI.2016.2593954).
- [9] T. Knopp, T. Viereck, G. Bringout, M. Ahlborg, A. von Gladiss, C. Kaethner, A. Neumann, P. Vogel, J. Rahmer, and M. Möddel. Mdf: Magnetic particle imaging data format, 2016. eprint: [arXiv:1602.06072](https://arxiv.org/abs/1602.06072).